



Universiteit
Leiden
The Netherlands

Molecular and cellular characterization of cardiac overload-induced hypertrophy and failure

Umar, S.

Citation

Umar, S. (2009, June 18). *Molecular and cellular characterization of cardiac overload-induced hypertrophy and failure*. Retrieved from <https://hdl.handle.net/1887/13860>

Version: Corrected Publisher's Version

License: [Licence agreement concerning inclusion of doctoral thesis in the Institutional Repository of the University of Leiden](#)

Downloaded from: <https://hdl.handle.net/1887/13860>

Note: To cite this publication please use the final published version (if applicable).

Chapter 6

Stem cells from rats with pulmonary hypertension reduce pulmonary parenchymal damage, medial hypertrophy of pulmonary arterioles, and right ventricular hypertrophy in rats with pulmonary hypertension

S. Umar
Y. P. de Visser
P. Steendijk
C. I. Schutte
E.H. Laghmani
G. T. M. Wagenaar
W. H. Bax
D. A. Pijnappels
D. E. Atsma
M. J. Schali
E. E. van der Wall
A. van der Laarse

Submitted for publication

Abstract

Background: Pulmonary arterial hypertension (PAH) is a chronic lung disease characterized by increased pulmonary artery pressure, pulmonary vascular damage and medial hypertrophy of pulmonary arterioles. Stem cell therapy may improve pulmonary damage in patients with PAH.

Purpose: To test the effects of treatment with bone marrow-derived mesenchymal stem cells (MSCs) obtained from donor rats with monocrotaline (MCT)-induced PAH to recipient rats with MCT-induced PAH on (i) pulmonary artery pressure, (ii) lung histology, (iii) pulmonary arteriolar diameters, and (iv) right ventricular (RV) hypertrophy. This model was chosen to mimic autologous stem cell therapy.

Methods: Female Wistar rats were divided in 4 groups, receiving either PBS (control, n=10), MCT (60 mg/kg, n=10), MCT (60 mg/kg) 14 days later followed by administration of 10^6 MSCs per rat i.v. (n=10), or 10^6 skin fibroblasts (SFs) per rat i.v. (n=10). MSCs were obtained from bone-marrow of PAH rats treated with MCT (60 mg/kg) for 28 days. SFs were obtained from healthy rats. At 28 days after MCT (or PBS) administration, the animal was sacrificed, lungs and heart were excised, weighed, fixed and examined by histology.

Results: At 28 days after MCT-treatment, rats had PAH (RV peak systolic pressure of 42 ± 17 vs. 27 ± 5 mmHg in control; $p < 0.02$), and increased lung weight (1.66 ± 0.32 vs. 0.96 ± 0.15 g in control; $p < 0.05$). Lung histology demonstrated severe narrowing of precapillary arterioles, thickening of arteriolar walls (3.4 times increased vs. control; $p < 0.001$), thickening of alveolar septa (3.5 times increased vs. control; $p < 0.001$), and increased RV mass (by 63%; $p < 0.01$). Treatment with MSCs for 14 days attenuated PAH (31 ± 4 mmHg; n.s. vs. MCT60; n.s. vs. control), and almost normalized lung weight (1.16 ± 0.24 g; $p < 0.05$ vs. MCT60), wall thickness of arterioles ($p < 0.01$ vs. MCT60), thickness of alveolar septa ($p < 0.01$ vs. MCT60), and RV hypertrophy ($p < 0.01$ vs. MCT60). In MCT-treated rats i.v. therapy with SFs from healthy rats had less beneficial effects than i.v. therapy with MSCs from PAH rats.

Conclusions: Intravenous administration of MSCs from donor rats with PAH to recipient rats with PAH decreased RV peak systolic pressure, pulmonary arteriolar narrowing, alveolar septum thickening, and RV hypertrophy. These results suggest that autologous stem cell therapy may help to alleviate cardiac and pulmonary symptoms in patients with PAH.

Introduction

Pulmonary arterial hypertension (PAH) is a chronic lung disease characterized by increased pulmonary artery pressure, pulmonary vascular damage and medial hypertrophy of pulmonary arterioles. In the current study we use a well-established model of experimental PAH induction in rats by a single injection of monocrotaline (MCT). MCT, a pyrrolizidine alkaloid derived from *Crotalaria spectabilis*, causes a pulmonary vascular syndrome in rats characterized by proliferative pulmonary vasculitis, PAH, and cor pulmonale. Current lines of evidence of the pathogenesis of MCT-induced pneumotoxicity indicate that MCT is activated to one or more reactive metabolites in the liver, particularly a MCT pyrrole called dehydromonocrotaline [1-3], and is then transported by red blood cells to the lung [4], where it initiates endothelial injury [5,6]. The endothelial injury does not appear to be acute cell death but rather a pathological condition that leads to smooth muscle cell proliferation in the media of pulmonary arteriolar walls by unknown mechanisms. The role of inflammation in the progression of MCT-induced pulmonary vascular disease is uncertain. Both perivascular inflammation and platelet activation have been proposed as processes contributing to the response of the vascular media [3]. The resulting lung lesions mimic the changes observed in lungs of the patients with PAH. There is a positive correlation between progressive PAH, thickening of the medial wall of small pulmonary arteries and arterioles, and RV hypertrophy as a function of time [7].

PAH is a difficult disease to treat and has been shown to be refractory to most of the conventional therapies. Many treatment modalities have been employed for treating PAH ranging from calcium channel blockers [8], phosphodiesterase inhibitors [9], endothelin receptor antagonists [10] to prostacyclin analogues [11], but still a standard treatment is lacking. Combination therapy has also been employed more recently [12], but still no definitive results have been obtained.

Stem cell therapy may constitute a new treatment modality for patients with PAH. Different modes of administration of stem cells including intravenous [13], intratracheal [14], and direct implantation of cells into the lungs [15] have been used. We have used the intravenous route of administration being a safe and feasible method of cell injection.

We hypothesize that when administered intravenously, the mesenchymal stem cells (MSCs) filter through the lungs and have a chance to engraft at the sites of lung parenchymal or vascular damage. Once these cells reside in damaged tissue, they start secreting 'pro-survival factors' such as growth factors or cytokines, hence helping improve the tissue's condition by paracrine mechanisms [16] or possibly by differentiating into endothelial or smooth muscle cells [17] and help to ameliorate pulmonary damage.

Although i.v. administration of bone marrow-derived MSCs to treat PAH has been studied already [13], our purpose was to treat recipient rats with MCT-induced PAH with bone marrow-derived MSCs obtained from donor rats with MCT-induced PAH, to mimic autologous stem cell transplantation. In this study we demonstrate that treatment of rats with PAH with MSCs from donor rats with PAH results in (i) lower pulmonary artery pressure, (ii) lower lung weight, (iii) less

abnormalities of pulmonary architecture, and (*iv*) less RV hypertrophy, compared to rats with PAH that were not treated with MSCs.

Materials and Methods

Animals

All animals were treated in accordance with the national guidelines and with permission of the Animal Experiments Committee of the Leiden University Medical Center. Eight-week-old female Wistar rats weighing 200-250 g (Harlan, Zeist, The Netherlands) were treated with MCT (Sigma-Aldrich, Zwijndrecht, The Netherlands) to produce pulmonary hypertension. Rats were randomly assigned to four groups. The animals received a single subcutaneous injection of MCT diluted in phosphate-buffered saline (PBS) (MCT60, 60 mg/kg body wt, $n = 10$) or the same dose of MCT followed 14 days later by intravenous injection into the jugular vein of 10^6 Dil-labeled mesenchymal stem cells (MCT+MSC, $n = 10$), or 10^6 Dil-labeled skin fibroblasts (MCT+SF, $n = 10$). Control (Cont) rats ($n = 10$) were injected with an equal volume of PBS. The animals were housed, two animals per cage, with a 12:12-h light-dark cycle and an unrestricted food and water supply. After 4 wk, RV pressure was measured, and the rats were sacrificed.

Haemodynamic measurements

At day 28 after MCT (or PBS) administration, RV pressure was measured as published previously [18]. Briefly, the rats were sedated by inhalation of a mixture of isoflurane (4%) and oxygen. Subsequently, general anesthesia was induced by intraperitoneal (i.p.) injection of a fentanyl-fluanison-midazolam mixture in a dose of 0.25 mL/100 g body weight. The mixture consisted of two parts Hypnorm (0.315 mg/mL fentanyl+10 mg/mL fluanison; Vital-Pharma, Maarheeze, the Netherlands): one part Dormicum (5 mg/mL midazolam; Roche, Mijdrecht, the Netherlands) and one part saline. The animals were placed on a controlled warming pad to keep body temperature constant. After a tracheotomy was performed, a cannula (18G, Biovalve, Vygon, Ecoen, France) was inserted, and the animals were mechanically ventilated using a pressure-controlled respirator and a mixture of air and oxygen. The animals were placed under a stereomicroscope (Zeiss, Hamburg, Germany). After a midsternal thoracotomy was performed, a combined pressure-conductance catheter (model FT212, SciSense, London, Ontario, Canada) was introduced via the apex into the RV and positioned towards the pulmonary valve. The catheter connected to a signal processor (FV898 Control Box, SciSense) and RV pressures were recorded digitally. All data were acquired at a sample rate of 2,000 Hz and analyzed off-line by dedicated software (SciSense).

Cell isolation

Mesenchymal stem cell isolation and culture

Four weeks after MCT treatment (60 mg/kg, $n=10$) adult donor rats were anesthetized with isoflurane and killed by i.v. injection of KCl (100 mmol/L). Femurs and tibiae were removed and cleaned of all connective tissue and attached muscles. The proximal ends were clipped and bones placed in microfuge tubes supported by plastic inserts cut from 200 μ L pipette tips. Microfuge tubes were briefly centrifuged at 13,000 rpm for 1 min. The marrow pellets were resuspended in 10 mL of growth medium [Dulbecco's modified Eagle's medium (DMEM; Invitrogen, Breda, the Netherlands), supplemented with 15% fetal bovine serum (FBS; Invitrogen), penicillin (50 U/L), streptomycin (50 μ g/L), and amphotericin B solution (0.25 μ g/mL; Sigma-Aldrich)] supplemented with 6% heparin (400 IE/mL). This suspension was centrifuged again at 1000 rpm for 10 min. Next, the pellet was resuspended in 7 mL of growth medium supplemented with 5.75 μ g/mL DNase I (Sigma-Aldrich). The cells were plated in 25-cm² culture flasks (Becton Dickinson, Franklin Lakes, NJ, USA) and the culture was kept in a humidified hypoxic incubator CO₂/O₂ (5%/5%) at 37°C. The non-adherent cells were replated after 6 h. Two days later, non-adherent cells were removed by changing the medium to 12 mL of fresh growth medium. The medium was refreshed twice a week until the primary cultures were confluent. The advantages of culturing MSCs in a hypoxic environment have been documented frequently [19-23].

Skin fibroblasts

Skin fibroblasts (SFs) were grown from pieces of skin of healthy rats anesthetized by excess CO₂ and killed by i.v. injection of KCl (100 mmol/L). Skin samples were transferred to porcine gelatin (Sigma-Aldrich)-coated flasks, and cultured in DMEM containing 100 U/mL penicillin, 100 μ g/mL streptomycin, and 10% fetal bovine serum (FBS, all from Invitrogen) in a normoxic incubator (20% O₂ and 5% CO₂) at 37°C. Outgrowth of cells was visible 2 days after culture initiation. Three days later the skin pieces were removed and the skin fibroblasts were detached with trypsin-EDTA solution (Invitrogen), and reseeded in new culture flasks. For intravenous infusion into rats which had had MCT administration 14 days earlier, we used passage 4-6.

Cell injection

Before injection, the cells were trypsinized and labelled with the viable fluorescent dye CM-Dil according to the manufacturer's recommendations (CellTracker™, Molecular Probes, Invitrogen). At day 14, each rat was fixed on its back, and anaesthetized with isoflurane. The jugular vein in the neck was prepared free. A venous catheter (20G, Biovalve) was introduced in the vein. Through this catheter 1 mL of cell suspension (10⁶ cells/mL) was injected slowly. This suspension contained MSCs from rats with MCT-induced PAH or SFs from healthy rats. After removal of the catheter, the vein was pressed for 5 min to allow closure of the puncture and the skin was closed. The control animals received i.v. injections of 1 mL of PBS.

Tissue preparations

After hemodynamic measurements, lungs and heart were removed, snap-frozen in liquid nitrogen, and stored at -80°C until isolation of RNA. For histology studies, the trachea was cannulated (18G, Biovalve), and the lungs were fixed *in situ* via the trachea cannula with buffered formaldehyde (4% paraformaldehyde in PBS, pH 7.4) at a pressure of 25 cm H_2O for 5 min. After removal of lungs and hearts, lungs were fixed (additionally) in formaldehyde for 24 h at 4°C , and embedded in paraffin after dehydration in a graded alcohol series and xylene.

Real-time RT-PCR

Total RNA was isolated from lung tissue homogenates using guanidium-phenol-chloroform extraction and isopropanol precipitation (RNA-Bee, Tel-Test Inc., Bio-Connect BV, Huissen, the Netherlands). The RNA sample was dissolved in RNase-free water and quantified spectrophotometrically. First-strand cDNA synthesis was performed with the SuperScript Choice System (Life Technologies, Breda, the Netherlands) by mixing 2 μg total RNA with 0.5 μg of oligo(dT)12-18 primer in a total volume of 12 μL . After the mixture was heated at 70°C for 10 min, a solution containing 50 mmol/L Tris-HCl (pH 8.3), 75 mmol/L KCl, 3 mmol/L MgCl_2 , 10 mmol/L DTT, 0.5 mmol/L dNTPs, 0.5 μL RNase inhibitor, and 200 U Superscript Reverse Transcriptase was added, resulting in a total volume of 20.5 μL . This mixture was incubated at 42°C for 1 h; total volume was adjusted to 100 μL with RNase-free water and stored at -80°C until further use. For *real-time* quantitative PCR, 1 μL of first-strand cDNA diluted 1:10 in RNase-free water was used in a total volume of 25 μL , containing 12.5 μL 2x SYBR Green PCR Master Mix (Applied Biosystems, Foster City, CA, USA) and 200 ng of each primer. Primers, designed with the Primer Express software package (Applied Biosystems), are:

Interleukin-6:	forward	5'-ATATGTTCTCAGGGAGATCTTGGAA-3'
	reverse	5'-TGCATCATCGCTGTTTCATACAA-3'
TNFα:	forward	5'-ACAAGGCTGCCCGACTAT-3'
	reverse	5'-CTCCTGGTATGAAGTGGCAAATC-3'
Endothelin-1:	forward	5'-TGTGCTCACCAAAAAGACAAGAA-3'
	reverse	5'-GGTACTTTGGGCTCGGAGTTC-3'
VEGF-A:	forward	5'-GCGGATCAAACCTCACCAA-3'
	reverse	5'-TTGGTCTGCATTACATCTGCTA-3'
NOS-2:	forward	5'-GCTGCATGTGACTCCATCGA-3'
	reverse	5'-TCTCCATTGCCCGAGTTTTT-3'
NOS-3:	forward	5'-CCCTGCCAACGTGGAGAT-3'
	reverse	5'-ATCAAAGCGGCCATTTCT-3'
Tenascin-C:	forward	5'-TCACAGCTCTCGATGGTCCAT-3'
	reverse	5'-TGGCCAAGGCTTCTGAGTCT-3'
MMP2:	forward	5'-CCCACGAAGCCTTGTTTACC-3'
	reverse	5'-GAAGCGGAACGGGAAGTTG-3'
MMP9:	forward	5'-TCCGCAGTCCAAGAAGATTTTC-3'
	reverse	5'-GCACCGTCTGGCCTGTGTA-3'
β-actin:	forward	5'-GGCTCCTAGCACCATGAAGATC-3'
	reverse	5'-GAGCCACCAATCCACACAGA-3'

PCR reactions, consisting of 95°C for 10 min (1 cycle), 94°C for 15 s, and 60°C for 1 min (40 cycles), were performed on an ABI Prism 7900 HT Fast Real Time PCR system (Applied Biosystems) of the Leiden Genome Technology Center. Data were analyzed with the ABI Prism 7900 sequence detection system software (version 2.2) and quantified with the comparative threshold cycle method with β -actin as a housekeeping gene reference [24].

Histochemical analysis

Fixed lung tissue, embedded in paraffin, was cut into 4- μ m-thick sections and stained with hematoxylin-phloxin-saffron for determination of thickness of alveolar septa.

Tracing the Dil-labeled stem cells in the lungs

Four μ m thick sections of lung tissue were deparaffinised in Ultraclear (Klinipath, Duiven, the Netherlands) and rehydrated in decreasing series of graded alcohols (100-25%), followed by two 5-min washes in distilled water and TBS (150 mmol/L NaCl, 10 mmol/L Tris-HCl, pH 8.0). Subsequently, nuclei were stained with 10 μ g/mL Hoechst 33342 solution (Molecular Probes, Invitrogen) for 10 min at room temperature. Sections were washed three times with TBS and mounted with Vectashield (Vector Laboratories, Burlingame, CA, USA).

Antibodies

Primary antibodies used were mouse anti α -smooth muscle actin (ASMA) antibody (S2547, Sigma-Aldrich), mouse anti-ED1 antibody (gift from Dr. E. de Heer, Department of Pathology, LUMC) to stain for interstitial monocytes/macrophages, mouse anti-myeloperoxidase (MPO) antibody (Thermo Fisher Scientific, Waltham, MA, USA) for neutrophil identification, and rabbit anti-CC10 antibody (C5828-03, United States Biological, Swampscott, MA, USA) to identify Clara cells.

Secondary HRP conjugated antibody were goat anti-mouse-IgG conjugated to HRP (sc2005, Santa Cruz Biotechnology, Santa Cruz, CA, USA), or goat anti-rabbit-IgG conjugated to HRP (sc2004, Santa Cruz Biotechnology). Substrate was 3,3'-diaminobenzidine (DAB)(Pierce, Perbio Science, Etten-leur, the Netherlands) or NovaRed (Vector Laboratories).

Immunoperoxidase staining protocol

Tissue was deparaffinized in Ultraclear two times for 10 min each, followed by 100% ethanol 2 times for 5 min each. The sections were rehydrated in decreasing graded alcohols (from 96% to 50%) for 3 min each and washed twice for 5 min each in distilled water and PBS. To inhibit endogenous peroxidase activity, the sections were incubated with 0.3% H₂O₂ in PBS for 20 min at room temperature. Next, the sections were boiled in 1.8% citrate buffer in a microwave for 12 min at 98°C. The next step was incubation in blocking solution, consisting of 5% bovine serum albumin (BSA) in PBS, for 1 hour at room temperature. Subsequently, sections were incubated with primary antibody diluted in PBS containing 1% BSA

and 0.05% Tween (100 μ L per sample), in a dilution of 1:100, overnight at room temperature. The sections were washed in PBS 3 times for 5 min each. Next, the sections were incubated with secondary antibody diluted in PBS containing 1% BSA and 0.05% Tween (100 μ L per sample), in a dilution of 1:200, for 60 min at room temperature. After washing, 100 μ L DAB was added to the sections (250 μ L of 10x DAB solution and 2250 μ L buffer (Pierce)) for 5 min, and washed again. Sections were stained in 1% hematoxylin for 1 min, and rinsed under running tap water for 10 min. In the end, to dehydrate the slides, sections were incubated in 50%, 70% and 96% ethanol for 3 min each, in 100% ethanol 2 times for 5 min, and in Ultraclear 2 times for 10 min each. Next, sections were mounted with D.P.X (BDH, Brunschwig Chemie, Amsterdam, the Netherlands), and examined under the microscope with light microscopy.

Microscopy

Stained slides were photographed using a microscope (Nikon Eclipse, Nikon Europe, Badhoevedorp, the Netherlands) equipped with 10x, 20x, 40x and 100x objectives and a digital camera (model DXM1800, Nikon). This microscope performed both light microscopy and fluorescence microscopy.

Quantitative image analysis

Quantitative image analysis was performed with Image-Pro Plus software (Media Cybernetics, Silver Spring, MD, USA). For determination of alveolar septum thickness hematoxylin-phloxin-saffron stained lung tissue was photographed at high magnification (100x). At locations distant from branch points and arterioles alveolar septum thickness was measured with calipers in Image-Pro Plus. For determination of precapillary arteriolar wall thickness, ASMA-stained lung tissue was photographed at high magnification (100x). Wall thickness of arterioles localized at branch points of alveolar septa was measured with calipers in Image-Pro Plus.

Assessment of RV hypertrophy

To quantify the degree of right ventricular hypertrophy hearts were harvested, followed by the removal of the left and right atrium. Hereafter the right ventricular free wall (RV) was dissected, weighted separately from the left ventricle (LV), including the interventricular septum (IVS), and frozen immediately in liquid nitrogen and stored at -80°C . RV mass is used as an indicator of right ventricular hypertrophy.

Statistical analysis

The effect of treatment (cell therapy with MSCs, cell therapy with SFs) was evaluated by one-way ANOVA followed by Bonferroni's *post-hoc* test. SPSS12 for Windows (SPSS Inc., Chicago, IL, USA) was used for statistical analysis. Differences were considered significant at $p < 0.05$. Values are represented by means \pm SD, unless stated otherwise.

Results

RV peak systolic pressure

At the end of the experimental period, RV peak systolic pressures were significantly higher in MCT60 group than in the control group, indicating the development of PAH (42 ± 17 vs. 27 ± 5 mmHg in control; $p < 0.02$). In MCT-treated rats that had been given cell therapy with MSCs, mean RV peak systolic pressure was attenuated (31 ± 4 mmHg) although not significantly different from MCT60, nor from control. In the MCT+SF group, the RV peak systolic pressure was 32 ± 6 mmHg, which was not significantly different from MCT60 nor from control (Figure 1).

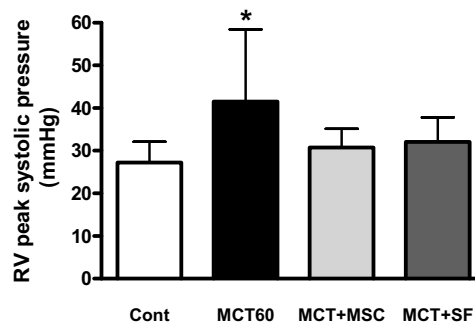


Figure 1. RV peak systolic pressures (mmHg) of Control, MCT60, MCT+MSC and MCT+SF groups are shown. Values are expressed as mean \pm SD (* $p < 0.05$ vs. Control).

Lung weights

Lung weight was 0.96 ± 0.15 g in control animals. Lung weight was significantly increased in the MCT60 group to 1.66 ± 0.32 g ($p < 0.05$ vs. control). With stem cell therapy, lung weight had decreased to 1.16 ± 0.24 g ($p < 0.05$ vs. MCT60). Lung weight in the MCT+SF group was 1.52 ± 0.20 g ($p < 0.05$ vs. control), which was not different from MCT60 (Figure 2). The increase in lung weight observed in the MCT60 and MCT+SF groups is symptomatic for an increased remodeling of lung tissue in these groups, rather than to pulmonary edema [18].

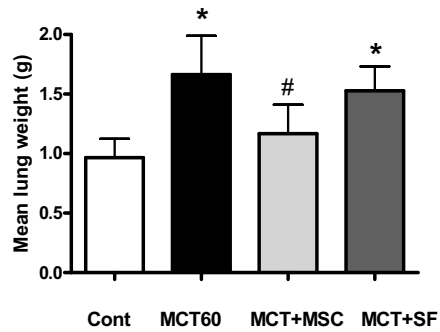


Figure 2. Lung weights (g) of Control, MCT60, MCT+MSC and MCT+SF groups are shown. Values are expressed as mean \pm SD (* $p < 0.05$ vs. Control, # $p < 0.05$ vs. MCT60).

RV hypertrophy

In MCT-treated rats RV mass had increased from 143 ± 26 mg to 233 ± 53 mg ($p < 0.05$). RV mass of MCT-treated rats that had received MSCs was 162 ± 25 mg ($p < 0.01$ vs. MCT60) which was not different from Control. In MCT-treated rats that had received SFs RV mass was 183 ± 33 mg ($p < 0.05$ vs. MCT60) which was not different from Control rats (Figure 3)..

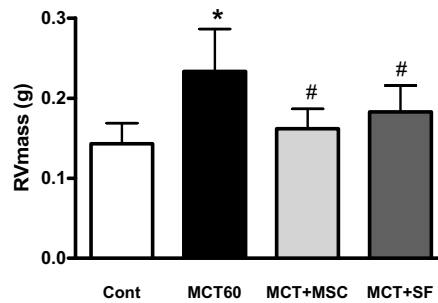


Figure 3. Right ventricular weight (RV mass) of Control, MCT60, MCT+MSC and MCT+SF groups are shown. Values are expressed as mean \pm SD (* $p < 0.05$ vs. Control, # $p < 0.05$ vs. MCT60).

mRNA in pulmonary tissue

Relative concentrations of mRNA encoding IL6, TNF α and MMP2 have increased in lungs of rats with MCT-induced PAH, although only significant for IL6 and MMP2 (Figure 4). However, mRNA encoding ET1 and VEGF-A had decreased significantly in lungs of rats treated with MCT. In the lungs of rats receiving cell therapy relative concentrations of mRNA did not differ, or only slightly, from those in rats of the MCT60 group. mRNA encoding NOS2 and NOS3 did not show changes between the experimental groups of rats (Figure 4).

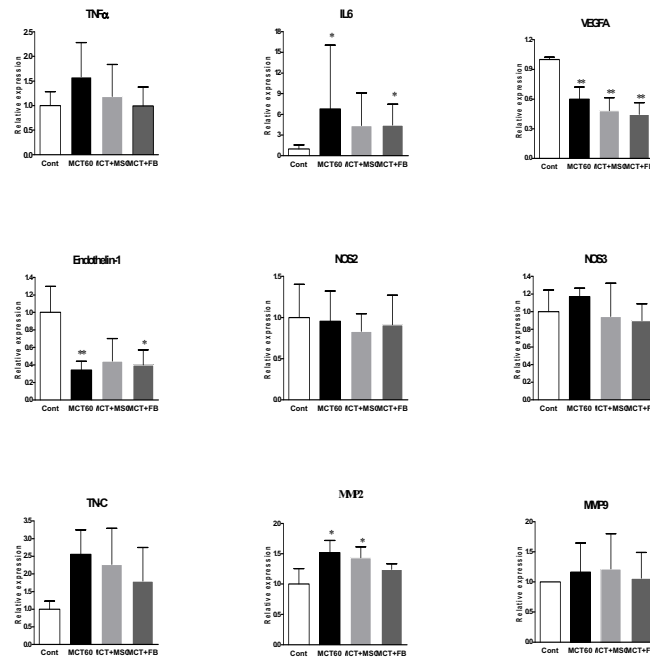


Figure 4. Right ventricular concentrations of mRNA encoding tumor necrosis factor- α (TNF α), interleukin-6 (IL-6), vascular endothelial growth factor-A (VEGFA), endothelin-1 (ET-1), nitric oxide synthase-2 (NOS2), nitric oxide synthase-3 (NOS3), tenascin-C (TN-C), matrix metalloproteinase-2 (MMP2) and matrix metalloproteinase-9 (MMP9). For each mRNA, myocardial concentration is normalized for the concentration found in hearts of PBS-treated rats (controls, Cont). * $p < 0.05$ vs. Cont (control), ** $p < 0.01$ vs. Cont (control)

Mean pulmonary arteriolar wall thickness

Mean pulmonary arteriolar wall thickness was significantly increased in MCT60 group to 343 ± 60 % ($p < 0.05$ vs. control). With MSC therapy, the arteriolar wall thickness had decreased to 120 ± 28 % ($p < 0.05$ vs. MCT60). The wall thickness in the MCT+SF group was 296 ± 35 % ($p < 0.05$ vs. control), which was not different from MCT60 (Figure 5). The increase in pulmonary arteriolar wall thickness observed in the MCT60 and MCT+SF groups represents arteriolar medial hypertrophy in these rats, which is apparently prevented largely by treatment with MSCs.

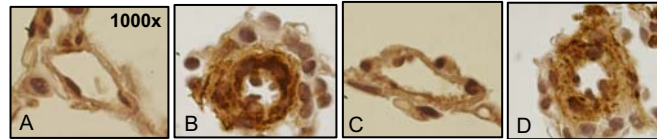


Figure 5a. Immunoperoxidase images of paraffin sections of lung tissue stained with anti α -smooth muscle actin antibody. Representative pulmonary arterioles of Control (panel A), MCT60 (panel B), MCT+MSC (panel C) and MCT+SF (panel D) are shown.

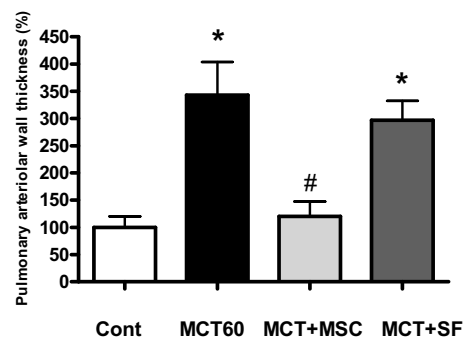


Figure 5b. Pulmonary arteriolar wall thickness (%) of Control, MCT60, MCT+MSC and MCT+SF groups are shown. Values are expressed as mean \pm SD (* $p < 0.05$ vs. Control, # $p < 0.05$ vs. MCT60).

Mean pulmonary alveolar septum thickness

Mean pulmonary alveolar septum thickness was significantly increased in the MCT60 group to 353 ± 56 % ($p < 0.05$ vs. control). With stem cell therapy, the alveolar septum thickness was only 109 ± 20 % ($p < 0.05$ vs. MCT60). Alveolar septum thickness in the MCT+SF group was 309 ± 28 % ($p < 0.05$ vs. control), which was not different from MCT60 (Figure 6). The increase in the mean pulmonary alveolar septum thickness observed in MCT60 and MCT+SF groups is prevented largely by treatment with MSCs.

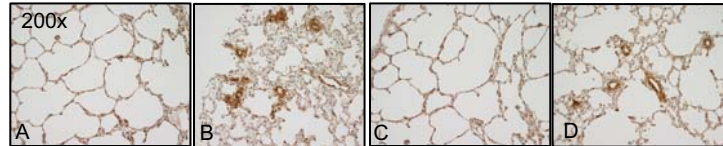


Figure 6a. Immunoperoxidase images of paraffin sections of lung tissue stained with anti α -smooth muscle actin antibody. Lung histology of Control (panel A), MCT60 (panel B), MCT+MSC (panel C) and MCT+SF (panel D) are shown.

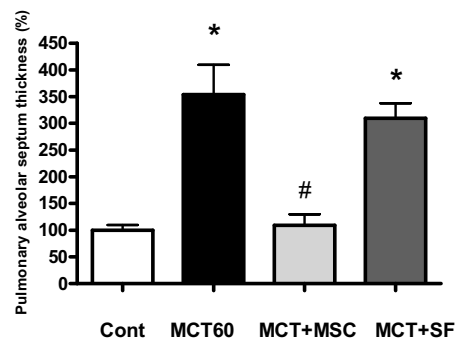


Figure 6b. Pulmonary alveolar septum thickness (%) of Control, MCT60, MCT+MSC and MCT+SF groups are shown. Values are expressed as mean \pm SD (* $p < 0.05$ vs. Control, # $p < 0.05$ vs. MCT60).

Recovery of Dil-labeled MSCs in the lung

In each rat that received cell therapy with MSCs (at day 14) the lungs were found to contain Dil-labeled MSCs at day 28 (Figure 7). Labeled MSCs were located in or near the pulmonary arterioles. They were not positive for CC10, thereby excluding the possibility that injected MSCs had differentiated into Clara cells.

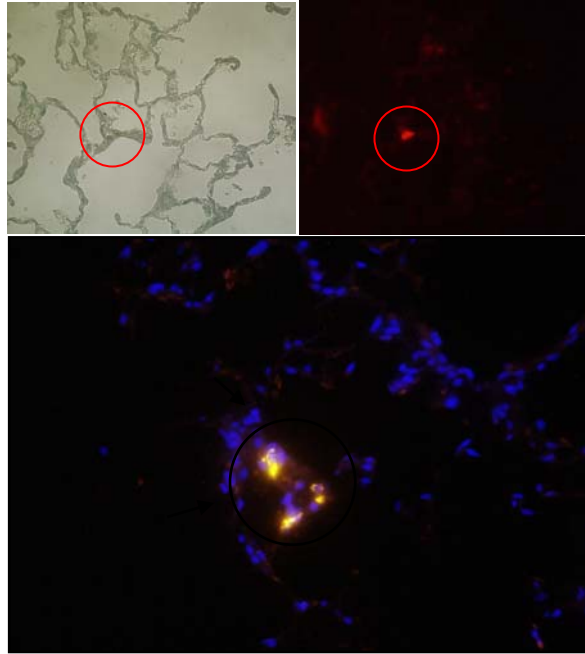


Figure 7. Fluorescence images of Dil-labeled MSCs in lungs acquired using 200x (top panels) and 400x (bottom panel) objectives. Dil-labelled MSCs are stained red, whereas nuclei are stained blue.

Abundance of ED1-positive and MPO-positive cells in lung tissue

Numbers of MPO-positive cells in lung tissue, nor numbers of ED1-positive cells in lung tissue differed between the experimental groups of rats (Figure 8).

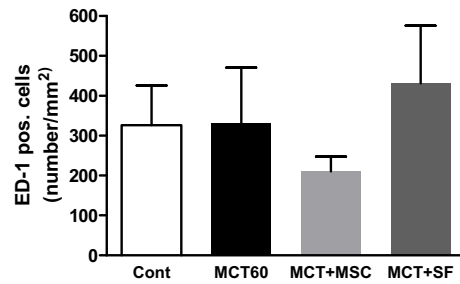


Figure 8a. Number of myeloperoxidase (MPO)-positive cells per image (0.34 mm²) of lung tissue from rats in 4 experimental groups. Per bar, 5 images have been scored. Indicated are mean values and SD.

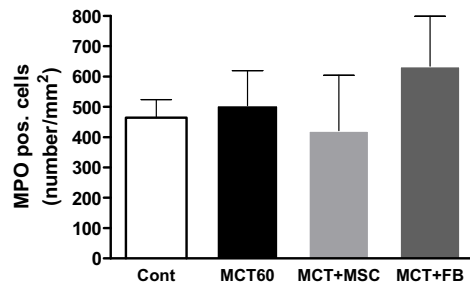


Figure 8b. Number of ED1-positive cells per image (0.34 mm²) of lung tissue from rats in 4 experimental groups. Per bar, 5 images have been scored. Indicated are mean values and SD.

Discussion

In the present study we have shown that i.v. injection of MSCs obtained from donor rats suffering from PAH into recipient rats with PAH has beneficial effects on lungs and heart, such as decreased RV peak systolic pressure, reduced pulmonary arteriolar narrowing and alveolar septum thickening, and less RV hypertrophy, compared to rats not receiving cell therapy.

MCT, a plant-derived toxin, causes endothelial cell injury, as observed in reduced expression of VEGF and endothelin-1, and subsequently an infiltration of mononuclear cells into the perivascular regions of arterioles and muscular arteries when injected i.v. in rats. These animals develop severe PAH after exposure to MCT [25]. Although typical plexiform lesions are not normally found in MCT-induced PAH, it is used as a standard model for PAH and primary pulmonary hypertension.

The important role of inflammation in this model has led to several studies focusing on immunosuppressive and anti-cytokine treatment, and, therefore, raises the question of how inflammation is involved in the installation and evolution of PAH lesions in humans.

Pathological changes in lungs of patients with PAH do not involve the whole pulmonary arterial tree, but remain restricted to certain vessel types. The concentric obliterative arteriopathy concerns muscular arteries of $\leq 500 \mu\text{m}$ in diameter, corresponding to the smaller arteries and their down-stream arterioles. Different and characteristic lesions, such as medial hypertrophy, intimal fibrosis, and typical plexiform lesions, as well as perivascular lymphocytic infiltrates are found [27,27]. Also Dorfmueller and coworkers reported that inflammatory mechanisms play a significant role in MCT-induced PAH in rats and pulmonary arterial hypertension of various origins in humans [28]. As for the MCT-model in the rat, typical plexiform lesions of smaller arteries are usually not found, but the primary importance of inflammation is illustrated by successful therapies using an interleukin-1 receptor antagonist [29] and antibodies to monocyte chemoattractant protein-1 [30]. In the present study we found significantly increased pulmonary expression of IL-6 in rats with MCT-induced PAH, which remained unaffected by cell therapy with SFs and with MSCs, although pulmonary IL6 mRNA concentration in MCT-treated rats that received MSCs was not significantly different from that in control lungs (Fig 4). MCT-induced endothelial cell dysfunction is associated with deregulated expression of vasoactive, mitogenic and proinflammatory mediators that may cause these changes [31,32]. Although we have stained the lung tissue for ED1 and MPO, we did not find ample evidence for interstitial accumulation of monocytes/macrophages and neutrophils in the lung, respectively. In the lungs of patients with pulmonary hypertension there is medial hypertrophy of arteries and increased pulmonary vascular resistance. In contrast to the lungs of control subjects, NOS was hardly expressed in the vascular endothelium of all type of vessels in the lungs of patients with pulmonary hypertension [33]. The arterial expression of NOS correlated inversely with the severity of histologic changes. The lack of NOS3-derived NO is responsible for proliferation of medial smooth muscle cells [34], which explains the simultaneous presence of, and interrelation between, lack of endothelial NOS

and arterial/arteriolar wall thickening. In the present study we found no indications of a downregulation of NOS3 induced by MCT without or with cell therapy.

In the lungs of patients with pulmonary hypertension endothelial expression of endothelin-1 (ET1) was abundant, predominantly in endothelial cells of pulmonary arteries with medial thickening and intimal fibrosis. At sites of increased ET1 immunoreactivity the ET1 mRNA concentration was high [35]. High levels of ET1 may induce proliferation of fibroblasts and increase the production of fibrous tissue *in vitro* [36]. In the present study, expression of ET1 in lung tissue of rats with MCT-induced PAH is markedly depressed, is unaffected by cell therapy with SFs, but has improved somewhat by cell therapy with MSCs.

In our study, we have observed remodeling of lung tissue in MCT-induced PAH as depicted by an increase in lung weights in MCT60 and MCT+SF groups (Fig. 2). The increase in lung weights observed in these groups is indicative for an increased ECM deposition in lung tissue in these groups, rather than pulmonary edema [18]. In addition, there was an increase in the mean alveolar septal thickness along with a higher incidence of discontinuous alveolar septa leading to larger alveolar spaces (Fig. 6). On further histological analysis, the mean pulmonary arteriolar wall thickness was significantly increased in MCT60 and MCT+SF groups (Fig. 5). With regard to the expression of MMPs in lung tissue, we found that MMP9 expression did not differ significantly between the groups, while MMP2 expression was significantly increased in MCT60 and MCT+MSC groups. Although TNC expression was increased in MCT60 group (1.6 times vs. control), the increase was not significant (Fig. 4). Increased expression of TNC has been shown to be associated with progression of clinical and experimental pulmonary hypertension [37,38]. Furthermore, MMP expression and activity are increased in experimental PAH [39]. Cell proliferation and ECM accumulation are also prominent features of idiopathic PAH. An important component of these changes is ECM remodeling, which results from a complex interplay between the synthesis and proteolysis of ECM constituents [40]. Hence any therapy having anti-remodeling effects may also be effective in treating PAH in the patients.

Many treatment options for PAH have been tested so far, but an effective therapy is lacking. Cell therapy constitutes a novel therapeutic option for PAH patients. Several groups have tested several cell types to treat experimental PAH, including endothelial progenitor cells [41], unfractionated bone marrow-derived cells [42,43], and mesenchymal stem cells (MSCs)[13]. MSCs are unique in possessing (*i*) a potential to differentiate into other cell types, and (*ii*) an ability to secrete paracrine factors leading to improvements in tissue injury [44]. Stem cell therapy using bone marrow-derived MSCs may actively replace differentiated cells that were damaged by MCT and/or contribute to tissue repair by secreting a wide variety of cytokines and growth factors. Generally the highest levels of engraftment are observed in tissues that are severely injured. Nagaya and coworkers recovered i.v. administered endothelial progenitor cells (EPCs) engrafted in pulmonary arterioles and capillaries of rats with MCT-induced PAH and differentiated endothelial cells [45]. With stem cell therapy we found anti-remodeling effects in the MCT+MSC group including a decrease in lung weights (Fig. 2), alveolar septal thickness (Fig. 6) and arteriolar wall thickness (Fig. 5), combined with an improvement in pulmonary architecture.

In the lungs we found most Dil-labeled MSCs engrafted in or near the arterioles (Fig. 7). Their therapeutic effect is, therefore, interpreted to originate from their paracrine effect, *i.e.* the production of cytokines and growth factors. These factors promote angiogenesis and may stop the proliferative thickening of arteriolar medial layers. I.v. administration of pulmonary artery-derived smooth muscle cells that were *in vitro* transduced with the VEGF-A gene was shown to have a substantial therapeutic effect in rats with MCT-induced PAH, whereas the use of the same cell type without gene transduction was without effect [46].

Apparently, the paracrine effects of intrapulmonary engrafted MSCs are more important than the differentiation of engrafted MSCs into vascular smooth muscle cells, endothelial cells, and/or Clara cells. With the anti-CC10 antibody we were unable to find any Dil-labeled MSC in the lung tissue that was CC10 positive. In contrast to the marked benefits of the therapy with i.v. MSCs, the effects obtained after injection with SFs were small, if present at all. Earlier Campbell and coworkers have used pulmonary artery-derived smooth muscle cells (PA-SMCs) injected i.v. together with MCT and found no therapeutic effect on pulmonary artery pressure [47]. If PA-SMCs were injected 2 weeks after MCT administration, cell therapy had no effect [46]. I.v. injected skin fibroblasts 3 days after MCT administration had no therapeutic effect as assessed 3 weeks later [41]. Using skin fibroblasts from healthy rats, injected i.v. in rats 2 weeks after MCT administration, we found no significant therapy effect on lung weight, arteriolar wall thickness, and alveolar septum thickness, although an unexplained therapy effect on RV mass is observed. Compared to injected MSCs, the injected SFs had slight therapeutic effects that may be ascribed to their inability to secrete large quantities of cytokines and growth factors.

Conclusion

In conclusion, i.v. administration of bone marrow-derived MSCs obtained from donor rats suffering from PAH into recipient rats with PAH decreases RV peak systolic pressure, pulmonary arteriolar narrowing, alveolar septum thickening, and RV hypertrophy. Based on these results, the use of autologous bone marrow-derived MSCs to treat PAH in humans is recommended.

Acknowledgements

Dr. J.W.A. van der Hoorn (TNO-Prevention & Health, Leiden) is gratefully acknowledged for staining lung tissue. The anti-ED1 antibody was a kind gift from Dr. E. de Heer (Department of Pathology, Leiden University Medical Center).

References

1. Butler WH, Mattocks AR, Barnes JM. Lesions in the liver and lungs of rats given pyrrole derivatives of pyrrolizidine alkaloids. *J Pathol* 1970; 100: 169-75.
2. Lafranconi WM, Huxtable RJ. Hepatic metabolism and pulmonary toxicity of monocrotaline using isolated perfused liver and lung. *Biochem Pharmacol* 1984; 33: 2479-84.
3. Wilson DW, Segall HJ, Pan LC, Lame MW, Estep JE, Morin D. Mechanisms and pathology of monocrotaline pulmonary toxicity. *Crit Rev Toxicol* 1992; 22: 307-25.
4. Lamé MW, Jones AD, Morin D, Wilson DW, Segall HJ. Association of dehydromonocrotaline with rat red blood cells. *Chem Res Toxicol* 1997; 10: 694-701.
5. Reindel JF, Hoorn CM, Wagner JG, Roth RA. Comparison of response of bovine and porcine pulmonary arterial endothelial cells to monocrotaline pyrrole. *Am J Physiol Lung Cell Mol Physiol* 1991; 261: L406-L414.
6. Reindel JF, Roth RA. The effects of monocrotaline pyrrole on cultured bovine pulmonary artery endothelial and smooth muscle cells. *Am J Pathol* 1991; 138: 707-19.
7. Ghodsi F, Will JA. Changes in pulmonary structure and function induced by monocrotaline intoxication. *Am J Physiol Heart Circ Physiol* 1981; 240: H149-H155.
8. Mawatari E, Hongo M, Sakai A, Terasawa F, Takahashi M, Yazaki Y, Kinoshita O, Ikeda U. Amlodipine prevents monocrotaline-induced pulmonary arterial hypertension and prolongs survival in rats independent of blood pressure lowering. *Clin Exp Pharmacol Physiol* 2007; 34:594-600.
9. Dony E, Lai Y, Dumitrascu R, Pullamsetti SS, Savai R, Ghofrani HA, Weissmann N, Schudt C, Flockerzi D, Seeger W, Grimminger F, Schermuly RT. Partial reversal of experimental pulmonary hypertension by phosphodiesterase 3/4 inhibition. *Eur Respir J* 2008;31:599-610.
10. Nishida M, Eshiro K, Okada Y, Takaoka M, Matsumura Y. Roles of endothelin ET_A and ET_B receptors in the pathogenesis of monocrotaline-induced pulmonary hypertension. *J Cardiovasc Pharmacol* 2004; 44:187-91.
11. Obata H, Sakai Y, Ohnishi S, Takeshita S, Mori H, Kodama M, Kangawa K, Aizawa Y, Nagaya N. Single injection of a sustained-release prostacyclin analog improves pulmonary hypertension in rats. *Am J Respir Crit Care Med* 2008; 177:195-201.
12. Clozel M, Hess P, Rey M, Iglarz M, Binkert C, Qiu C. Bosentan, sildenafil, and their combination in the monocrotaline model of pulmonary hypertension in rats. *Exp Biol Med* 2006; 231: 967-73.
13. Kanki-Horimoto S, Horimoto H, Mieno S, Kishida K, Watanabe F, Furuya E, Katsumata T. Implantation of mesenchymal stem cells overexpressing endothelial nitric oxide synthase improves right ventricular impairments caused by pulmonary hypertension. *Circulation* 2006; 114(suppl I); I-181-I-185.
14. Baber SR, Deng, Master RG, Bunnell BA, Taylor BK, Murthy SN, Hyman AL, Kadowitz PJ. Intratracheal mesenchymal stem cell administration attenuates monocrotaline induced pulmonary hypertension and endothelial dysfunction. *Am J Physiol Heart Circ Physiol* 2007; 292: H1120-H1128.
15. Takahashi M, Nakamura T, Toba T, Kajiwara N, Kato H, Shimizu Y. Transplantation of endothelial progenitor cells into the lung to alleviate pulmonary hypertension in dogs. *Tissue Eng* 2004; 10: 771-9.
16. Kinnaird T, Stabile E, Burnett MS, Shou M, Lee CW, Barr S, Fuchs S, Epstein SE. Local delivery of marrow-derived stromal cells augments collateral perfusion through paracrine mechanisms. *Circulation* 2004;109:1543-9.
17. Al-Khaldi A, Al-Sabti H, Galipeau J, Lachapelle K. Therapeutic angiogenesis using autologous bone marrow stromal cells: Improved blood flow in a chronic limb ischemia model. *Ann Thorac Surg* 2003;75:204-9.

18. Hessel MH, Steendijk P, den Adel B, Schutte CI, van der Laarse A. Characterization of right ventricular function after monocrotaline-induced pulmonary hypertension in the intact rat. *Am J Physiol Heart Circ Physiol* 2006; 291: H2424-H2430.
19. Lennon DP, Edmison JM, Caplan AI. Cultivation of rat marrow-derived mesenchymal stem cells in reduced oxygen tension: Effects of in vitro and in vivo osteochondrogenesis. *J Cell Physiol* 2001;187:345-55.
20. Grayson WL, Zhao F, Bunnell B, Ma T. Hypoxia enhances proliferation and tissue formation of human mesenchymal stem cells. *Biochem Biophys Res Comm* 2007;358:948-53.
21. Buravkova LB, Anokhina EB. Effect of hypoxia on stromal precursors from rat bone marrow at the early stage of culturing. *Bull Exp Biol Med* 2007; 143: 411-3.
22. Rosova I, Dao M, Capoccia B, Link D, Nolte JA. Hypoxic preconditioning results in increased motility and improved therapeutic potential of human mesenchymal stem cells. *Stem Cells* 2008;26:2173-82.
23. Hu X, Yu SP, Fraser JL, Lu Z, Ogle ME, Wang J-A, Wei L. Transplantation of hypoxia-preconditioned mesenchymal stem cells improves infarcted heart function via enhanced survival of implanted cells and angiogenesis. *J Thorac Cardiovasc Surg* 2008;135:799-808.
24. Pfaffl MW. A new mathematical model for relative quantification in real-time RT-PCR. *Nucleic Acids Res* 2001; 29: e45.
25. Nishimura T, Faul JL, Berry GJ, Veve I, Pearl RG, Kao PN. 40-O-(2-Hydroxyethyl)-rapamycin attenuates pulmonary arterial hypertension and neointimal formation in rats. *Am J Resp Crit Care Med* 2001; 163: 498-502.
26. Tuder RM, Groves B, Badesch DB, Voelkel NF. Exuberant endothelial cell growth and element of inflammation are present in plexiform lesions of pulmonary hypertension. *Am J Pathol* 1994; 144: 275-85.
27. Pietra GG. The pathology of primary pulmonary hypertension. In: Rubin L, Rich S, eds. *Primary pulmonary hypertension*. New York, Marcel Dekker, 1997; pp. 19-61.
28. Dorfmueller P, Perros F, Balabanian K, Humbert M. Inflammation in pulmonary arterial hypertension. *Eur Respir J* 2003; 22: 358-63.
29. Voelkel NF, Tuder RM, Bridges J, Arend WP. Interleukin-1 receptor antagonist treatment reduces pulmonary hypertension generated in rats by monocrotaline. *Am J Respir Cell Mol Biol* 1994;11:664-75.
30. Kimura H, Kasahara Y, Kurosu K, Sugito K, Takiguchi Y, Terai M, Mikata A, Natsume M, Mukaida N, Matsushima K, Kuriyama T. Alleviation of monocrotaline-induced pulmonary hypertension by antibodies to monocyte chemoattractant and activating factor/monocyte chemoattractant protein-1. *Lab Invest* 1998;78:571-81.
31. Loscalzo J. Endothelial dysfunction in pulmonary hypertension. *N Engl J Med* 1992; 327: 117-9.
32. Lopes AA, Maeda NY, Goncalves RC, Bydlowski SP. Endothelial cell dysfunction correlates differentially with survival in primary and secondary pulmonary hypertension. *Am Heart J* 2000; 139: 618-23.
33. Giaid A, Saleh D. Reduced expression of endothelial nitric oxide synthase in the lungs of patients with pulmonary hypertension. *N Engl J Med* 1995;333:214-21.
34. Cornwell TL, Arnold E, Boerth NJ, Lincoln TM. Inhibition of smooth muscle cell growth by nitric oxide and activation of cAMP-dependent protein kinase by cGMP. *Am J Physiol Cell Physiol* 1994;267:C1405-C1413.
35. Giaid A, Yanagisawa M, Langleben D, Michel RP, Levy R, Shennib H, Kimura S, Masaki T, Duguid WP, Stewart DJ. Expression of endothelin-1 in the lungs of patients with pulmonary hypertension. *N Engl J Med* 1993;328:1732-9.
36. Kahaleh MB. Endothelin, an endothelial-dependent vasoconstrictor in scleroderma. Enhanced production and profibrotic action. *Arthritis Rheum* 1991;34:978-83.

37. Jones PL, Cowan K, Rabinovitch M. Tenascin-C, proliferation and subendothelial accumulation of fibronectin in progressive pulmonary vascular disease. *Am J Pathol* 1997; 150:1349-60.
38. Jones PL, Rabinovitch M. Tenascin-C is induced with progressive pulmonary vascular disease in rats and is functionally related to increased smooth muscle cell proliferation. *Circ Res* 1996;79:1131-42.
39. Frisdal E, Gest V, Vieillard-Baron A, Levame M, Lepetit H, Eddahibi S, Lafuma C, Harf A, Adnot S, d'Ortho M. Gelatinase expression in pulmonary arteries during experimental pulmonary hypertension. *Eur Respir J* 2001;18:838-45.
40. Archer S, Rich S. Primary pulmonary hypertension: a vascular biology and translational research "Work in progress". *Circulation* 2000;102:2781-91.
41. Zhao YD, Courtman DW, Deng Y, Kugathasan L, Zhang Q, Stewart DJ. Rescue of monocrotaline-induced pulmonary arterial hypertension using bone marrow-derived endothelial-like progenitor cells. Efficacy of combined cell and eNOS gene therapy in established disease. *Circ Res* 2005; 96: 442-50.
42. Sahara M, Sata M, Morita T, Nakamura K, Hirata Y, Nagai R. Diverse contribution of bone marrow-derived cells to vascular remodeling associated with pulmonary arterial hypertension and arterial neointimal formation. *Circulation* 2007;115:509-17.
43. Raoul W, Wagner-Ballon O, Saber G, Hulin A, Marcos E, Giraudier S, Vainchenker W, Adnot S, Eddahibi S, Maitre B. Effects of bone marrow-derived cells on monocrotaline- and hypoxia-induced pulmonary hypertension in mice. *Resp Res* 2007;8:8.
44. Passier R, Mummery C. Origin and use of embryonic and adult stem cells in differentiation and tissue repair. *Cardiovasc Res* 2003; 58: 324-35.
45. Nagaya N, Kangawa K, Kanda M, Uematsu M, Horio T, Fukuyama N, Hino J, Harada-Shiba M, Okumura H, Tabata Y, Mochizuki N, Chiba Y, Nishioka K, Miyatake K, Asahara T, Hara H, Mori H. Hybrid cell-gene therapy for pulmonary hypertension based on phagocytosing action of endothelial progenitor cells. *Circulation* 2003;108:889-95.
46. Campbell AIM, Zhao Y, Sandhu R, Stewart DJ. Cell-based gene transfer of vascular endothelial growth factor attenuates monocrotaline-induced pulmonary hypertension. *Circulation* 2001;104:2242-8.
47. Campbell AIM, Kuliszewski MA, Stewart DJ. Cell-based gene transfer to the pulmonary vasculature. Endothelial nitric oxide synthase overexpression inhibits monocrotaline-induced pulmonary hypertension. *Am J Respir Cell Mol Biol* 1999;21:567-75.

